ISSN 1066-3622, Radiochemistry, 2007, Vol. 49, No. 1, pp. 20–24. © Pleiades Publishing, Inc., 2007.
Original Russian Text © S.V. Beshta, E.V. Krushinov, V.I. Al'myashev, S.A. Vitol', L.P. Mezentseva, Yu.B. Petrov, D.B. Lopukh, N.A. Lomanova, V.B. Khabenskii, M. Barrachin, S. Hellmann, K. Froment, M. Fisher, W. Tromm, D. Bottomley, V.V. Gusarov, 2007, published in Radiokhimiya, 2007, Vol. 49, No. 1, pp. 20–24.

Phase Transformation in the Binary Section of the UO_2–FeO–Fe System

S. V. Beshta[a], E. V. Krushinov[a], V. I. Al'myashev[b], S. A. Vitol'[a], L. P. Mezentseva[b], Yu. B. Petrov[c], D. B. Lopukh[c], N. A. Lomanova[b], V. B. Khabenskii[a], M. Barrachin[d], S. Hellmann[e], K. Froment[f], M. Fisher[e], W. Tromm[g], D. Bottomley[h], and V. V. Gusarov[b]

[a] *Aleksandrov Research Technological Institute, Sosnovyi Bor, Leningrad oblast, Russia*
[b] *Grebenshchikov Institute of Silicate Chemistry, Russian Academy of Sciences, St. Petersburg, Russia*
[c] *St. Petersburg State Electrotechnical University, St. Petersburg, Russia*
[d] *Institut de Radioprotection et Surete Nucleaire, Paris, France*
[e] *Framatome Atomic Nuclear Plant, Erlangen, Germany*
[f] *Commissariat a l'Energie Atomique, Grenoble, France*
[g] *Institut für Kern- und Energietechnik, Forschungszentrum Karlsruhe, Karlsruhe, Germany*
[h] *Institute of Transuranium Elements, Joint Research Center, Karlsruhe, Germany*

Received October 25, 2005

Abstract—Phase transformations in the oxide binary section of the UO_2–FeO–Fe ternary system were studied. The melting onset point of the UO_2–FeO heterogeneous system (1335 ± 5°C) was determined and the fusion curve of this system was constructed. The limiting solubility of FeO in the UO_2 solid solution was measured. The changes in crystal parameters in formation of the solid solution were determined. Uranium dioxide was found to be insoluble in the wüstite phase (FeO).

PACS numbers: 61.10.Nz, 81.30.Dz
DOI: 10.1134/S1066362207010031

Data on phase and chemical transformation in systems containing uranium oxide are important for nuclear power engineering [1], since UO_2 is used mainly as a fuel. Since the equipment for localization of molten reactor core at severe accidents contains iron oxides [2–4], the data on phase transformations in the system in question are important for analysis of physicochemical processes occurring at such accidents.

Published data on phase transformations in the U–Fe–O system in relation to the temperature and partial oxygen pressure are scarce [1, 5–9]. The oxide part of this system lying in the U_3O_8–UO_2–Fe_2O_3–Fe_3O_4 tetrahedron was studied to the greatest extent [8, 9]. Using the model suggested in [10], we calculated the phase diagram of the UO_2–FeO system. The calculated eutectic point (~1350°C) is observed at the UO_2 concentration of ~5 mol %.

The lack of detailed data on phase transformations in the U–Fe–O system, especially in the oxide part of the system at the boundary with the metallic phases, i.e., in the UO_2–FeO–Fe subsystem, is due to experimental difficulties in the study of this system [1].

Therefore, systematic experimental study of phase transformations in the UO_2–FeO oxide system coexisting with the metal phase (Fe) is an urgent problem.

EXPERIMENTAL

We used UO_2 (depleted uranium containing less than 0.7% ^{235}U), FeO of chemically pure grade, and Fe of ultrapure grade.

Samples of the UO_2–FeO–Fe system were prepared by induction melting in a cold crucible (IMCC) on Rasplav-2 and Rasplav-3 units in an argon flow. The units and the procedure for melting in a cold crucible were described in detail in our previous papers [11, 12].

To prepare crystalline iron oxide with the wüstite structure ($Fe_{1-x}O$) of the composition closest to the FeO stoichiometry, we used, in accordance with the Fe–Fe_2O_3 phase diagram, metallic iron as a getter in 1 wt % excess with respect to the total weight of the sample. Under these conditions, iron oxide crystallizes in the form of nonstoichiometric phase

$Fe_{0.938}O$. Hereinafter this phase will be conventionally denoted as FeO.

To perform X-ray phase analysis and to determine the unit cell parameters, we used powder X-ray diffraction patterns recorded on a DRON-3 diffractometer (FeK_α radiation).

The chemical composition of the samples was determined by spectrophotometric and gas-volumetric procedures described in [13–15] and by X-ray photoelectron spectroscopy (XPS) on a SPARK 1-M spectrometer.

The microstructure and elemental analysis of the multiphase samples and individual phases were determined by scanning electron microscopy (SEM) and energy-dispersive X-ray spectral microanalysis (EDXSMA) on a CamScan MV 2300 or AVT-55 scanning electron microscope equipped with an Oxford Link microprobe attachment. The determination error of the element content was ~0.3 wt %.

Thermal transformations in the UO_2–FeO–(Fe) system were studied by differential thermal analysis (DTA) on a SETARAM SETSYS Evolution 2400 derivatograph under an atmosphere of high-purity Ar. Temperatures of thermal effects were determined from the onset of the DTA peaks, which, in turn, were determined from the intersection of the tangent to branches of the baseline and of the curve of the thermal effect. The analysis was performed in corundum or platinum crucibles. The sample weight was approximately 30 mg. The heating and cooling rates were 5°C min^{-1}.

Melting and crystallization in the examined systems were also studied by visual polythermal analysis (VPA) using the IMCC procedure [16] and in Galakhov microfurnace [17]. The point of crystallization onset of the melt in the system (liquidus temperature) was determined by the VPA IMCC procedure [16]. The point of melting onset (solidus temperature) and the temperature of complete melting of all components of the system (liquidus temperature) were determined by the VPA procedure in a Galakhov microfurnace [18].

The samples with eutectic composition were prepared by slow crystallization of the melt under the IMCC conditions. Under these conditions, the liquid approaching the eutectic composition is pushed off by the crystallization front of the liquid in the course of crystallization of the highest-melting component. The eutectic crystallization zone was identified by the characteristic microstructure of the ingot.

To determine the limiting solubility of FeO in the variable-composition phase of uranium dioxide, solid solution UO_2(FeO) was contacted for a long time with a melt of the composition close to the eutectic.

RESULTS AND DISCUSSION

The study of the phase transformations in the oxide subsystem of the UO_2–FeO–Fe system was performed at the UO_2 concentration ranging from 3.9 to 67.5 mol %.

The macro- and microstructure of the crystallized melt of the initial mixture melted by the IMCC procedure was shown in Fig. 1. All the samples contain eutectic crystallization zones along with the crystallization zones of the highest-melting component (Fig. 1). As determined by XSMA, the UO_2 content in the eutectic formed in different samples is 3.98–0.12 mol %. The crystallization onset temperatures of the examined samples measured by VPA IMCC are presented in Fig. 2.

Parts of the samples prepared by IMCC procedure were taken and studied by DTA and VPA in a Galakhov microfurnace.

The thermal analysis curve of the sample containing 7.0 ± 0.5 mol UO_2 is shown in Fig. 3a (Al_2O_3 crucible). The DTA curve recorded in the course of heating has two sharp endothermic peaks at 1335 and 1379°C assigned to the onset of melting and complete melting of the sample. Two exothermic peaks at 1393 and 1348°C, observed in the course of cooling, are due to the onset of crystallization and complete crystallization of the sample. The difference in the temperatures of these effects measured on heating and cooling of the sample cannot be due to supercooling, since the crystallization onset temperature measured by DTA is higher than the melting point. This difference may be caused by reaction of the sample with the crucible material (aluminum oxide). It should also be noted that the first endothermic peak is a superposition of two thermal effects: onset of melting of the UO_2–FeO system at 1335°C and reaction of the sample with Al_2O_3 (crucible material) at 1346°C. Since Al_2O_3 is relatively high-melting substance, the melting point of the sample increases. Thus, the melting onset temperature of the sample should be taken as 1335°C.

To make the assignment of the results of thermal analysis more definite, a sample containing ~4 mol % UO_2 was studied by DTA in a platinum crucible. In this case, the oxide phases do not react with the crucible material and hence the composition of the oxide system does not change in the course of its

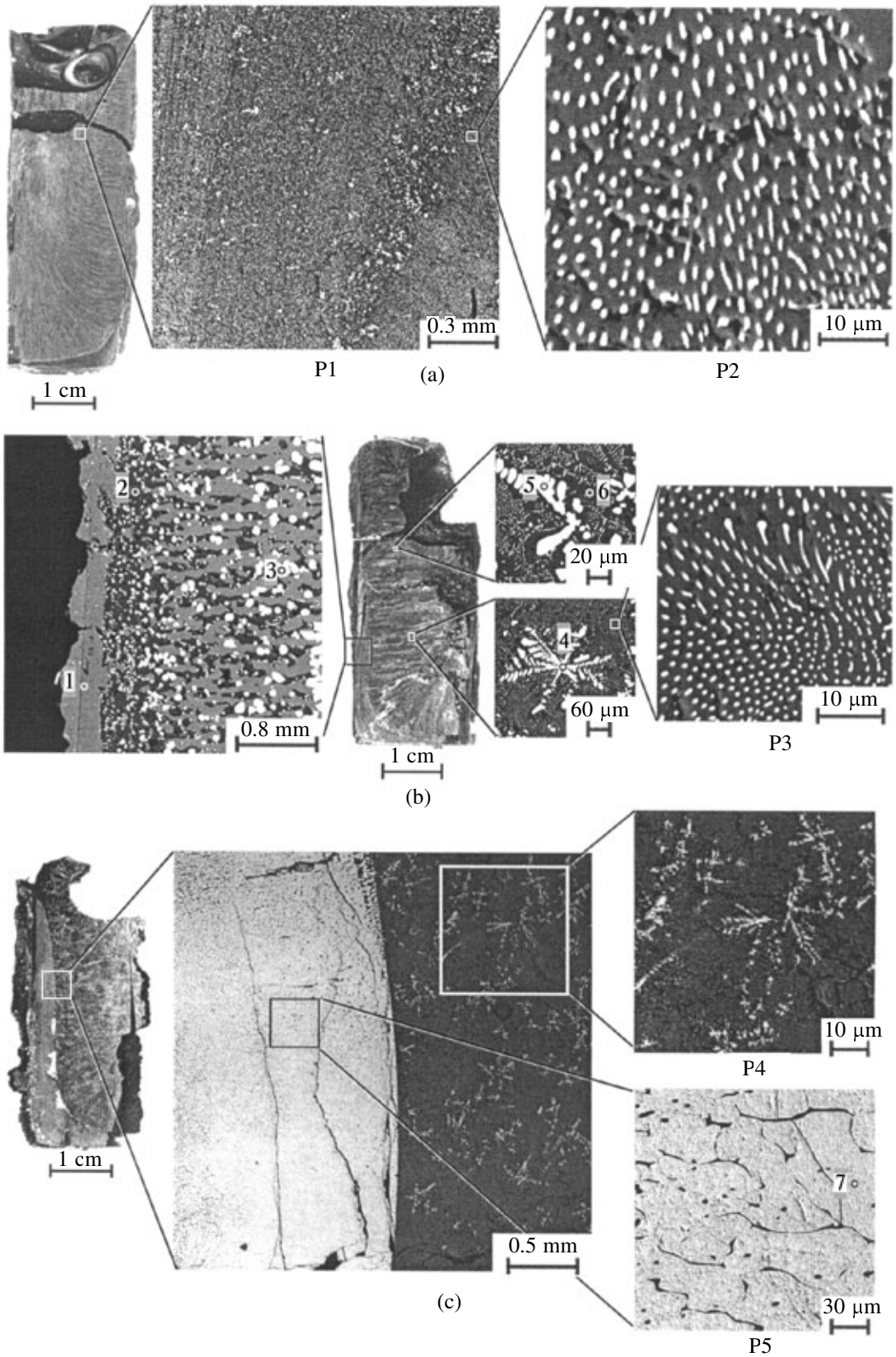

Fig. 1. Micrographs of crystallized samples of the UO_2–FeO system containing (a) 3.9 mol % UO_2; (b) 7.0 mol % UO_2 (the sample was quenched from 1850°C); (c) 21.0 mol % UO_2 (the sample was prepared by drawing of the ingot from the inductor).

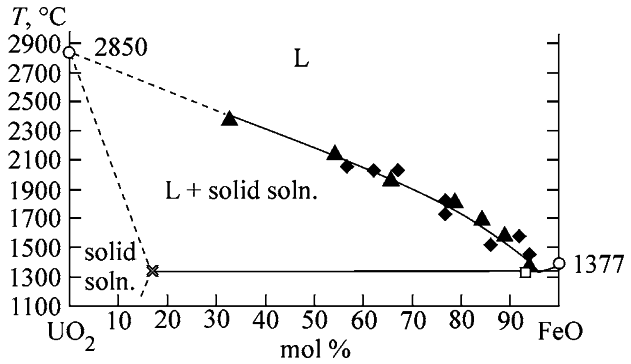

Fig. 2. Phase diagram of the UO_2–FeO system (inert atmosphere). Circles, data of [16]; triangles, data obtained by VPA IMCC; rhombs, data obtained in Galakhov microfurance; squares, results of DTA; and crosses, results of IMCC/XSMA.

melting. The DTA curve (Fig. 3b) contains three peaks at 1313, 1334, and 1354°C. The thermal effect starting at 1334°C is probably due to eutectic melting. The peak at 1354°C is assigned to the liquidus temperature. Since the composition of the oxide system does not change, the crystallization point of the melt should be equal to the melting onset temperature, which is observed in Fig. 3b. The broad thermal effect starting at 1313°C (heating) is probably due to the reaction of the crucible material (Pt) with iron present in the sample as a getter.

Solid solution of uranium dioxide UO_2(FeO) is present in all the samples prepared by crystallization of molten UO_2–FeO–(Fe) system, whereas UO_2 is almost insoluble in the wüstite phase (Fig. 1; see table). However, grains of UO_2(FeO) solid solution present in most of crystalline samples are too small to be determined by XSMA. This is due to eutectic or fast dendrite crystallization (Fig. 1a and 1b). In addition, UO_2(FeO) solid solution decomposes on cooling to form a thin layer of FeO around UO_2 grains (Fig. 1a, see table, zone 6). This is clearly caused by a decrease in the solubility of FeO in the UO_2 phase with decreasing temperature. To determine the limiting solubility of FeO in UO_2 more accurately, we grew UO_2(FeO) solid solution coexisting with the melt of the composition close to the eutectic (Fig. 1b, see table). For this purpose we used a sample containing 21.0 mol % UO_2. A thick layer of UO_2(FeO) solid solution that crystallized in this sample allows more accurate determination of the limiting solubility of FeO in UO_2 (Fig. 1b, see table). It should be noted that FeO separates in the form of a thin layer around UO_2(FeO) grains after annealing of this sample at temperatures corresponding to the solidus of this composition (Fig. 1c). The powder X-ray diffraction pat-

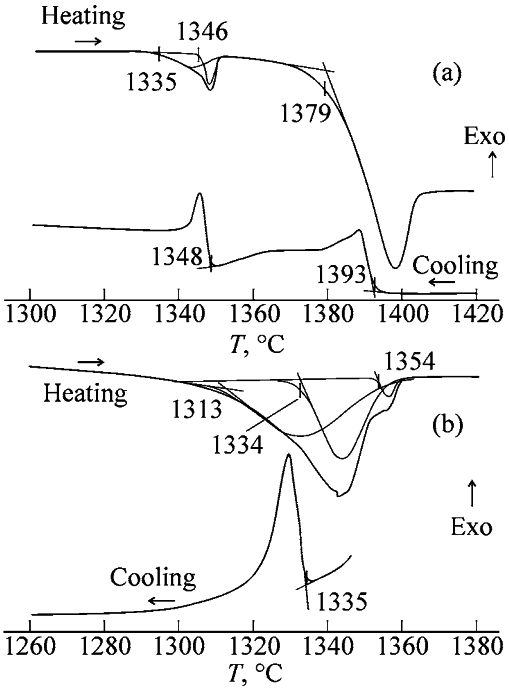

Fig. 3. DTA curves for the UO_2–FeO system: (a) sample containing 7.0 mol % UO_2 (inert atmosphere, corundum crucible); (b) sample containing approximately 4 mol % UO_2 (inert atmosphere, platinum crucible).

tern of the sample taken from the crystallization region of UO_2(FeO) solid solution (Fig. 1c) contains reflections of FeO along with the reflection of UO_2(FeO) (Fig. 4). Thus, UO_2(FeO) solid solution partially de-

Chemical composition of the zones outlined in Fig. 1

UO_2 content in the sample, mol %	Examined zone	Content, mol %	
		UO_2	FeO
3.9	P1	4.0	96.0
	P2	4.1	95.9
7.0	1	100% Fe	
	2	–	100
	3	96.1	3.9
	4	96.6	3.4
	5	95.5	4.5
	6	–	100
	P3	3.7	96.3
21.0	P4	4.3	95.7
	P5	83.3	16.7
	7*	~95	~5

* Calculated from the chemical composition of the P5 zone and the volume fractions of the phases coexisting in the P5 zone [UO_2(FeO) and FeO].

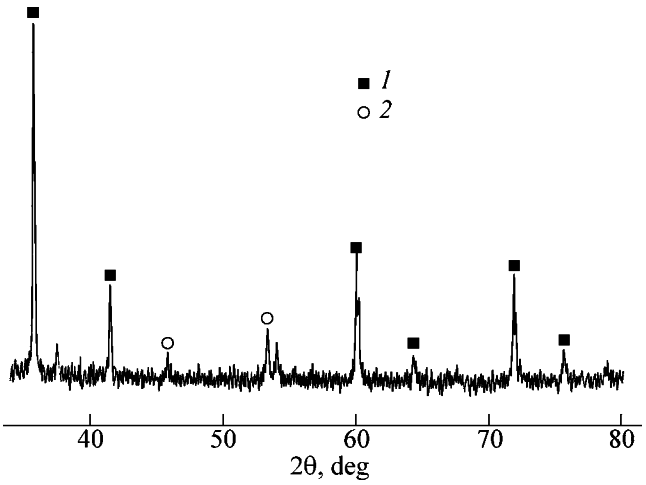

Fig. 4. X-ray pattern of the sample shown in Fig. 1b (P5 zone). (*1*) UO_2(FeO) and (*2*) FeO (wüstite).

composes on cooling to form the wüstite phase (FeO) on the grain boundaries.

The limiting solubility of FeO (16.7 mol %) determined by XSMA (Fig. 1c) refers to the temperature of the melt (1350°C) coexisting with solid UO_2(FeO). The limiting solubility of FeO in UO_2, determined by extrapolation of the line passing through the point of 1350°C and 16.7 mol % FeO to the eutectic temperature, is 17.0 mol % FeO (Fig. 2).

As determined by powder X-ray diffraction analysis, the unit cell volume of the UO_2 solid solution containing 5 mol % FeO (see table, area 7) is lower by 0.4% than that of UO_2 (the unit cell parameter of UO_2 is 5.4682 [19], and the unit cell parameter of UO_2(FeO) containing 5 mol% FeO is 5.4601 ± 0.0002 Å).

ACKNOWLEDGMENTS

This study was financially supported by ISTC (project no. 1950.2 CORPHAD).

REFERENCES

1. Voronov, N.M., Sofronova, R.M., and Voitekhova, E.A., *Vysokotemperaturnaya khimiya okislov urana i ikh soedinenii* (High-Temperature Chemistry of Uranium Oxides and Their Compounds), Moscow: Atomizdat, 1971.
2. Gusarov, V.V., Al'myashev, V.I., Beshta, S.V., et al., *Teploenergetika*, 2001, no. 9, pp. 22–24.
3. Gusarov V.V., Al'myashev, V.I., Saenko, I.V., et al., RF Patent no. 2 206 930, Published 20.06.2003, Priority of 02.04.2002.
4. Gusarov, V.V., Al'myashev, V.I., Khabenskii, V.B., et al., *Zh. Ross. Khim. O–va*., 2005, vol. 49, no. 4, pp. 17–28.
5. Bykov, M.A. and Uspenskaya, I.A., *Zh. Neorg. Khim*., 2003, vol. 48, no. 10, pp. 1715–1717.
6. Darken, L.S. and Gurry, R.W., *J. Am. Chem. Soc*., 1945, vol. 67, pp. 1398–1412.
7. Michaud, G.G., *Can. Met. Quart*., 1966, vol. 5, no. 4, pp. 355–365.
8. Kosulina, G.I., *Diagrammy sostoyaniya tugoplavkikh oksidov: Spravochnik: Dvoinye sistemy* (Phase Diagrams of High-Melting Oxides: Handbook: Binary Systems), Grebenshchikov, R.G., Ed., Leningrad: Nauka, 1991, part 5.
9. Evans, W.D.J. and White, J., *Trans. Brit. Ceram. Soc*., 1964, vol. 63, no. 12, pp. 705–724.
10. Epstein, L.F. and Howland, W.H., *J. Am. Ceram. Soc*., 1953, vol. 36, no. 10, pp. 334–335.
11. Petrov, Yu.B., *Induktsionnaya plavka okislov* (Induction Melting of Oxides), Leningrad: Energoatomizdat, 1983.
12. Lopukh, D., Bechta, S., Pechenkov, A., et al., in *Proc. ICONE 8: 8th Int. Conf. on Nuclear Engineering*, Baltimore, Maryland (USA), April 2–6, 2000, report ICONE-8139.
13. Markov, V.K., Vernyi, E.A., Vinogradov. A.V., et al., *Uran. Metody ego opredeleniya* (Uranium. Methods of Its Determination), Markov, V.K., Ed., Moscow: Atomizdat, 1964, 2nd ed.
14. Ryabchikov, D.I. and Senyavin, M.M., *Analiticheskaya khimiya urana* (Analytical Chemistry of Uranium), Moscow: Akad. Nauk SSSR, 1962.
15. Luk'yanov, V.F., Savvin, S.B., and Nikol'skaya, I.V., *Zh. Anal. Khim*., 1960, vol. 15, no. 3, pp. 311–314.
16. Petrov, Yu.B., Beshta, S.V., Vitol', S.A., et al., in *Materialy Mezhdunarodnoi konferentsii "Aktual'nye problemy teorii i praktiki induktsionnogo nagreva"* (Proc. Int. Conf. "Urgent Problems of Theory and Practice of Induction Heating"), St. Petersburg (Russia), May 25–26, 2005, pp. 161–169.
17. Galakhov, F.Ya., in *Sovremennye metody issledovaniya silikatov i stroitel'nykh materialov* (Modern Procedures for Studing Silicates and Building Materials), Moscow: Gosstroiizdat, 1961, p. 178.
18. Toropov, N.A. and Galakhov, F.Ya., *Izv. Akad. Nauk SSSR, Otd. Khim. Nauk*, 1956, no. 2, pp. 158–161.
19. ASTM, Card 5-550.